

# DESIGN OF THE PEP-II INTERACTION REGION SEPTUM QUADRUPOLE

J. Osborn, J. Tanabe, D. Yee, F. Younger, Lawrence Berkeley National Laboratory<sup>†</sup>

## Abstract

The PEP-II QF2 magnet is one of the final focus quadrupoles for the Low-Energy Ring (LER) and utilizes a septum aperture to accommodate the adjacent High-Energy Ring (HER) beamline. The LER lattice design specification calls for an extremely high field quality for this magnet. A conventional water-cooled copper coil and laminated steel core design was selected to allow adjustment in the excitation. The close proximity between the LER and HER beamlines and the required integrated quadrupole strength result in a moderately high current density septum design. The QF2 magnets are imbedded in a confined region at each end of the BaBar detector, thus requiring a small magnet core cross section. Pole face windings are included in the QF2 design to buck the skew octupole term induced by the solenoidal fringe field that leaks out of the detector. Back-leg windings are included to buck a small dipole component induced by the lack of perfect quadrupole symmetry in this septum design. 2D pole contour optimization and 3D end chamfers are used to minimize harmonic errors; a separate permanent-magnet Harmonic Corrector Ring compensates for remaining field errors. The design methods and approach, 2D and 3D analyses, and the resulting expected magnet performance are described in this paper.

## 1. REQUIREMENTS

The QF2 magnet along with the Q1, Q4, and Q5 magnets require the highest field quality of any magnets in PEP-II. The lattice requirements for the QF2 magnet combine high field quality with moderately high field strength and places the magnet in a congested region at each end of the BaBar detector. A permanent magnet design option was investigated in addition to the conventional design. The conventional design utilizing water-cooled copper coils and a laminated steel core was selected to allow adjustment in the excitation. Table I gives a summary of design requirements[1].

## 2. DESIGN PARAMETERS

The QF2 inboard end is about 3.1 meters from the interaction point. This places the magnet in a part of the lattice where the LER and HER beamlines are very close together, about 9.5 cm apart at the inboard end of QF2. In addition, the shape of the LER beam stay clear is

changing and its center is shifting over the length of the magnet, particularly at the inboard end.

Table I. Design requirements for QF2.

Nominal gradient [T/m]	7.7
Adjustment [%]	+3.5/-5
Effective length [m]	0.62
Allowed multipoles, main aperture, bn/b2 @ 4.23 cm	$\leq 1 \times 10^{-4}$
Allowed multipoles, septum aperture, bn @ 2.2 cm [T-m]	$\leq 2 \times 10^{-4}$

These considerations led to the selection of a quadrupole bore aperture radius of 47.8 mm with a 3x3 coil package of 5 mm square conductor. The core length was determined based on the required effective length and an estimate of the fringe integral including the shortening due to the end chamfers.

To achieve the required field strength in this tight package, a moderately high current density of 52 Amps/mm<sup>2</sup> and ample cooling is required. Though two-turn water circuits would achieve the desired cooling, single-turn circuits were selected for a lower ambient temperature within the support raft and to reduce the required cooling flow velocity. Table II summarizes the QF2 design parameters. Note that only 8 turns are energized in the 3x3 package; this is discussed below.

## 3. MECHANICAL DESIGN

Though utilizing conventional water-cooled copper coils and a laminated steel core, the QF2 design incorporates several additional features to meet its demanding requirements. Figures 1 and 2 show 3D representations which point out many of these features.

Table II. Design parameters for QF2.

Design gradient [T/m]	8.47
Core length [m]	0.61
Bore radius [mm]	47.8
Estimated efficiency [%]	96
Design excitation [Amp-Turns]	8021
Turns per coil	8
Design current [A]	1003
Design current density [A/mm <sup>2</sup> ]	52
Magnet resistance [mΩ]	52.6
Magnet power [kW]	52.9
Conductor size [mm]	5.0
Conductor hole diameter [mm]	2.5
Conductor corner radius [mm]	1.0
Cooling circuits per coil	8
Length per circuit [m]	1.7
Design pressure [mPa] / [psi]	2.07 / 30
Flow velocity [m/s] / [ft/s]	4.4 / 14.5
Magnet flow [l/s] / [gpm]	0.7 / 11
Temperature rise [°C]	18.2

<sup>†</sup>Work supported in part by the US Department of Energy under contract number DE-AC03-76SF00098.

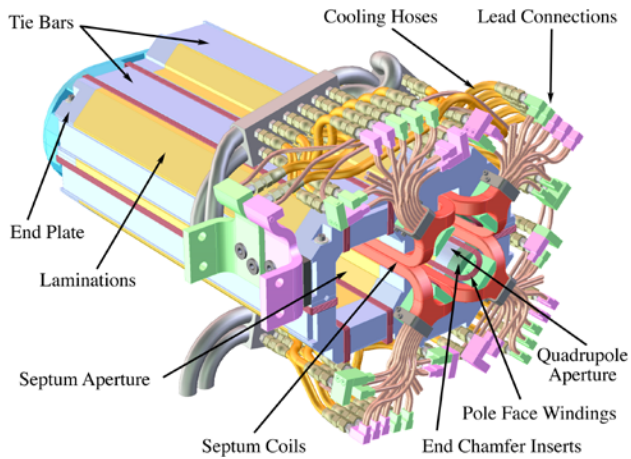


Fig. 1. Outboard from detector end of QF2.

In addition to the main quadrupole coils, there are three sets of trim windings. Back-leg trim windings are used to compensate for a small dipole and sextupole term in the quadrupole aperture, which is due to a small flux imbalance arising from the non-quadrupole symmetry in this design. 2D magnetic analyses were used to verify that when the back-leg trim windings are excited to the proper level (which is proportional to the main coil excitation), the magnet behaves like a symmetric quadrupole. Pole-face windings are used to induce a skew octupole term in the quadrupole aperture to buck the skew octupole term induced by the solenoidal field leaking out of the detector. Similarly, septum aperture windings are used to buck a skew-dipole term induced in the septum aperture by the detector's fringe field.

The QF2 design also incorporates a field-clamp with two bores at the inboard end of the magnet. The purpose of the field clamp is to absorb some of the solenoidal leakage field from the detector. In addition, the main aperture in the field clamp may be shaped so as to induce a skew octupole of the opposite sign to that induced in the core[2]. As yet unproved, this technique is promising as it potentially corrects for skew octupole passively without inducing higher order harmonics as do the pole-face windings.

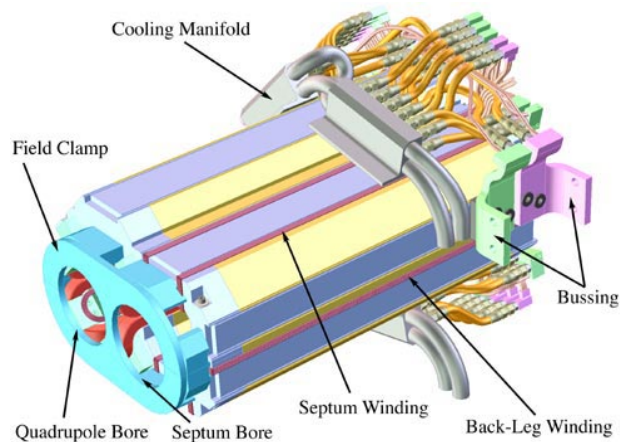


Fig. 2. Inboard towards detector end of QF2.

Since the shaped bore would be four-fold symmetric, only allowed harmonics are introduced, most notably  $N=6$ . So slightly different end-chamfers may be required.

#### 4. 2D MAGNETIC ANALYSES

Because the good field radius of 4.23 cm is large compared to the bore radius of 4.78 cm, there is not enough pole overhang to allow 2D optimization utilizing only pole bumps. Additionally, since the septum coil is tightly constrained in size and position, the coil is close to the aperture. Consequently conductor position has a significant effect on the multipole content. These factors led to a design in which a combination of conductor displacement into the aperture, the deactivation of one of the conductors in the nominal 3x3 package, and pole corner bumps were all used to achieve the desired field quality requirements. Figure 3 shows a close up cross-section of the coil and pole corner.

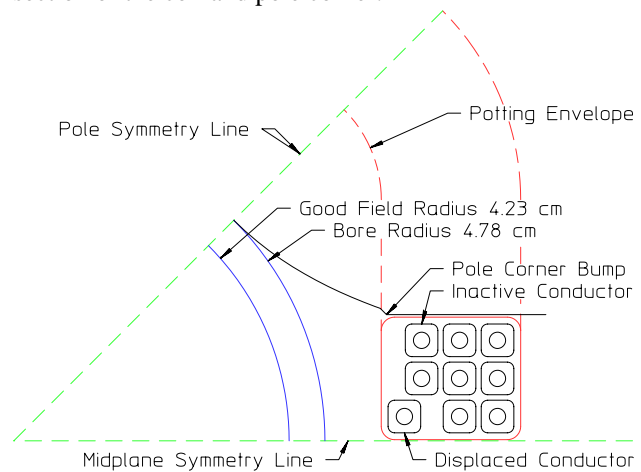


Fig. 3. Close-up view of coil and pole corner.

The pole corner bump geometry was selected to allow installation and removal of the coils and simultaneously to provide 45 degree flats for convenient measurements between opposing poles in the assembled magnet. The distance that this corner is pulled into the aperture from a nominally hyperbolic pole contour was used as one parameter in the 2D optimization.

It was determined that a very helpful reduction in the  $N=6$  term resulted when the conductor closest to the pole corner was deactivated. The displacement of the midplane conductor closest to the aperture was used as the second parameter in the 2D optimization. The complete 2D optimization strategy combines the conductor deactivation with a suitably sized pole corner bump and a suitable displacement of the midplane conductor.

In order to determine the optimal pole corner bump size and midplane conductor displacement, a grid study was performed using the Poisson/Superfish group of codes[3]. A series of iso-contours were calculated from interpolations of the grid cases for values of constant multipole content. The iso-contours show combinations

of bump size and conductor displacement where a given normalized multipole has a value of zero,  $1 \times 10^{-4}$ , or  $-1 \times 10^{-4}$ . For a given multipole, the band between these extremes can be interpreted as the locus of acceptable designs. The optimum combination can be determined from where the bands of  $N=6$ , 10, and 14 cross in the same region. Figure 4 shows the results of this study at the nominal excitation. Other grids were created using a variety of materials and excitations to determine that the design was insensitive to these changes. The final selected combination is where the  $N=10$  and  $N=14$  zero iso-contours cross. This leaves a residual  $N=6$  term of about  $1 \times 10^{-4}$  which will be trimmed along with the fringe field using end chamfers.

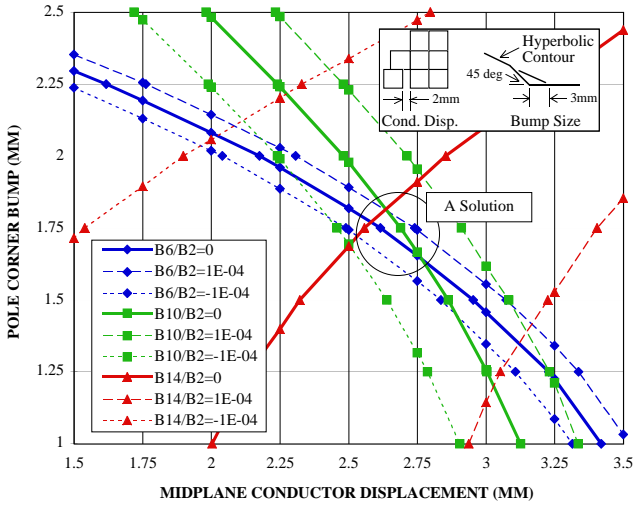


Fig. 4. 2D multipole iso-contours for various pole bumps and conductor displacements, nominal excitation, normalized @ 4.23 cm radius.

### 5. 3D MAGNETIC ANALYSES

To verify that the proposed chamfer inserts are large enough to allow trimming of the fringe field and the residual  $N=6$  from the 2D portion of the magnet, a similar grid study was performed in 3D for a series of simple notch end chamfers. The two parameters varied for these chamfers are the height along the pole axis (X-Y Direction) and the longitudinal depth (Z Direction). Figure 5 shows the notch depth and height convention.

The 2D Poisson performance with optimum pole bump and midplane conductor displacement was used to model the central 51 cm of 2D body harmonics, while the 3D integrated performance for the remaining fringe portion of the field was modeled with Amperes<sup>®</sup>[4]. Figure 6 shows the results of this study in format similar to Figure 4. A solution is evident where the bands of  $\pm 1 \times 10^{-4}$  for the various integrated normalized multipoles cross. The actual final 3D end chamfer geometry will be determined empirically after the magnet is built, by means of rotating coil measurements. It is expected that the required allowed multipole content of  $\leq 1 \times 10^{-4}$  will be achieved with careful fabrication and trimming.

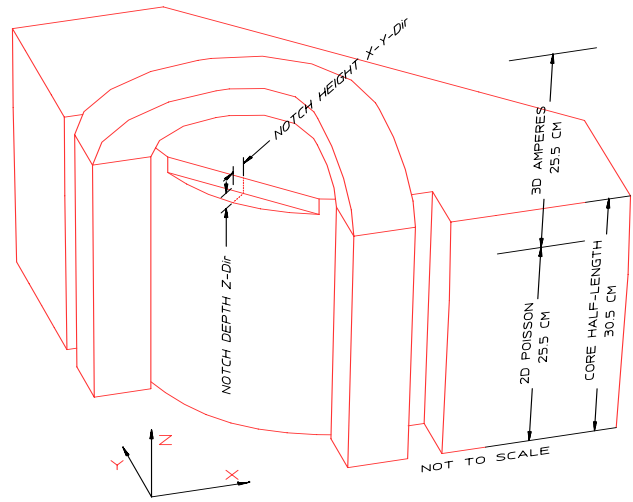


Fig. 5. Notch chamfer convention.

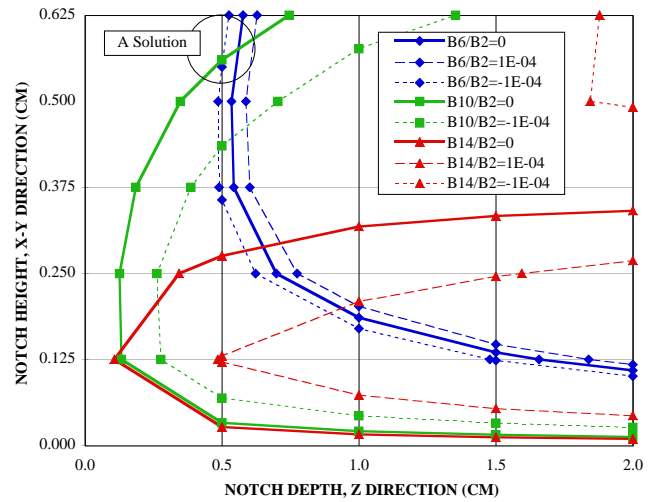


Fig. 6. 3D integrated multipole iso-contours for various notch end chamfers, nominal excitation, normalized @ 4.23 cm radius.

### 6. ACKNOWLEDGMENTS

The authors would like to thank all of the individuals working on the Interaction Region in PEP-II. This magnet is tightly constrained in many ways. The final design would not be possible without the professional cooperation between many competing interests in several collaborating laboratories.

### REFERENCES

- [1] PEP-II: An Asymmetric B Factory, Conceptual Design Report, June 1993.
- [2] Supplement to: Magnetic Field Calculation in the BaBar Detector, by S. Mikhailov et al., BaBar Note, December 25, 1996.
- [3] Poisson/Superfish Group of Codes, maintained by Los Alamos National Laboratory, contact: Robert Ryne, (505) 667-2839.
- [4] Amperes<sup>®</sup> Integrated Engineering Software, 46-1313 Border Place, Winnipeg, Manitoba, Canada, R3H0X4.